Nuclear Materials and Energy 36 (2023) 101476

Contents lists available at ScienceDirect

Nuclear Materials and Energy

journal homepage: www.elsevier.com/locate/nme

Post-mortem and in-situ investigations of magnetic dust in ASDEX Upgrade

M. De Angeli [a,*], V. Rohde [b], P. Tolias [c], S. Ratynskaia [c], F. Brochard [d], C. Conti [e], M. Faitsch [b], B. Kurzan [b], D. Ripamonti [f], the ASDEX Upgrade Team [1], the EUROfusion MST1 Team [2]

[a] Institute for Plasma Science and Technology - CNR, Via R. Cozzi 53, 20125 Milan, Italy
[b] Max–Planck-Institut für Plasmaphysik, Boltzmannstr. 2, 85748, Garching, Germany
[c] Space and Plasma Physics - KTH Royal Institute of Technology, Teknikringen 31, 10044 Stockholm, Sweden
[d] Université de Lorraine, Institut Jean Lamour, UMR 7198 CNRS, 54000 Nancy, France
[e] Institute of Heritage Science - CNR, Via R. Cozzi 53, 20125 Milano, Italy
[f] Institute of Condensed Matter Chemistry and Energy Technologies - CNR, Via R. Cozzi 53, 20125 Milan, Italy

ARTICLE INFO

Keywords:
Magnetic dust
Mobilization
Dust in tokamaks
ASDEX Upgrade

ABSTRACT

Pre-plasma mobilization of magnetic dust can be an important issue for future fusion reactors where plasma breakdown is critical. A combined on-line and off-line study of magnetic dust in ASDEX Upgrade is reported. Post-mortem collection revealed similar composition and morphology compared to other tokamaks, but the overall amount was much smaller. Optical and IR camera diagnostics excluded dust flybys prior to plasma start-up. The negative detection is discussed in light of the magnetic dust properties, the strength of mobilizing forces and the temporal evolution of the magnetic field.

1. Introduction

Mobilization has been nowadays recognized as an important aspect of dust transport and survivability in fusion devices [1,2]. Targeted cross-machine dust collection activities have provided evidence of the presence of a significant fraction of ferromagnetic and strongly paramagnetic particulates in the dust inventory of tokamaks (TEXTOR [3,4], FTU [5–7], Alcator C-Mod [6,7], COMPASS [6,7], DIII-D [6], EAST [8]), up to 27wt% depending on plasma-facing component (PFC) composition, cleaning protocols during shutdown and plasma operations.

In stark contrast to non-magnetic dust, magnetic particulates can be mobilized during, or even before, discharge start-up under the action of magnetic moment forces [9]. To date not enough attention has been paid to the occurrence and possible consequences of the pre-plasma remobilization of magnetic dust. In the perspective of the use of stainless steel for the ITER diagnostic first wall [10] and of reduced activation ferritic martensitic (RAFM) steel [11] in future fusion reactors such as DEMO [12], a fraction of magnetic dust could interfere with the breakdown phase of these devices, that is already known to be critical.

ASDEX Upgrade (AUG) operates with tungsten coated PFCs. It is the only European tokamak that features magnetic P92 steel and Eurofer steel tiles, which cover a part of the heat shield, aiming to improve our understanding of the effects of steel-induced magnetic perturbations on the plasma conditions, magnetic probe measurements and vessel integrity [13,14]. From the point of view of RAFM-like material use, AUG is the closest DEMO-like wall tokamak. Thus, AUG is the ideal fusion device for magnetic dust studies. Here, we present some preliminary results on the characteristics of magnetic dust in AUG and its possible mobilization before the beginning of plasma discharges.

2. Experimental approach

The experimental approach is based on experience gained from the study of magnetic dust in FTU, where the pre-plasma remobilization of magnetic dust due to the external magnetic field was first observed [9]. The same combined on-line and off-line strategy was followed in AUG. The on-line study aimed at verifying the existence of fly-by dust during the beginning of the plasma discharges. It was carried out by means of IR cameras and an optical diagnostic based on Mie scattering of laser light. The off-line study aimed at analyzing the chemical composition and morphology of magnetic dust after post-mortem collection from the vessel. It was carried out by means of Scanning Electron Microscopy (SEM), Energy-Dispersive X-ray (EDX) spectroscopy, and X-ray Diffraction (XRD) spectroscopy.

The *optical diagnostic* operated at the beginning of the 2022 experimental campaign, in a parasitic mode, utilizing two lines of the

* Corresponding author.
E-mail address: marco.deangeli@istp.cnr.it (M. De Angeli).
[1] See the author list of U. Stroth et al., NF 62 (2022) 042006.
[2] See the author list of B. Labit et al., NF 59 (2019) 086020.

https://doi.org/10.1016/j.nme.2023.101476
Received 13 June 2023; Received in revised form 21 July 2023; Accepted 25 July 2023
Available online 29 July 2023

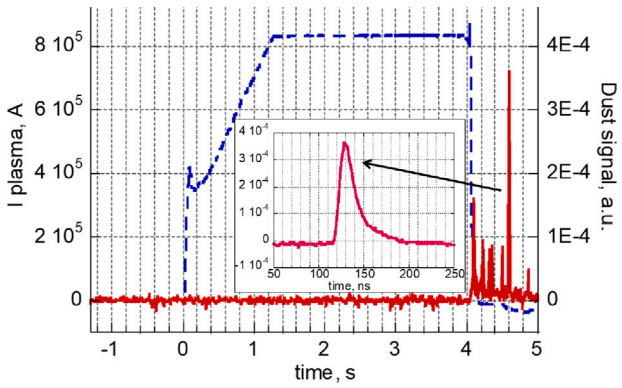

Fig. 1. Example of a dust signal acquired by the optical diagnostic during discharge #40256 (red line), which was terminated with a plasma disruption, along with the plasma current signal (blue dashed line). The insert shows the raw data of the optical diagnostic, sampled at 1 GS/s, of one of the detected dust particles. (For interpretation of the references to color in this figure legend, the reader is referred to the web version of this article.)

"core" view of the Thomson Scattering system (TS), covering the mid plane and the divertor regions of the vessel (between channels 5&6 and between channels 15&16 respectively, see Fig. 1 of Ref. [15]). Scattered light was detected by a photo diode, equipped with a laser line filter at 1064 nm. The dust signal acquisition was triggered −1.3 s before the discharges and recorded by the same fast acquisition system (synchronized with the laser shots) used by TS. The Nd-YAG laser pulses had a 10 ns duration, 1 J energy, 20 Hz frequency. A detailed description of the TS system can be found in Ref. [15]. Discharges stored in the AUG database were analyzed with a Python code, that scans the optical diagnostic signals for $t < 0$ s and evaluates an average background noise level (for any single shot). Peaks stronger than five times the average noise level and with a full width at half maximum (FWHM) between 5 ns and 40 ns are listed in a output table. The correspondence between peaks and laser shots is guaranteed by the hardware synchronization between the triggers of the lasers and of the signal acquisition system of the optical diagnostic. These peaks are manually verified to exclude any possible false positives. A classical example of dust signature as revealed by the optical diagnostic is shown in Fig. 1. This diagnostic was on-line from discharge #40235 to #41570; the last pulse prior to shutdown.

AUG is equipped with several *IR cameras* which cover a wide section of the vessel. The cameras considered in the present investigation are mounted in sectors 7&9 and image the mid plane and divertor regions, respectively. For the purpose of this study, these cameras were triggered −4.378 s before the discharges in order to detect any possible passage of mobilized magnetic dust. The videos were processed by applying dedicated temporal and spatial filters. It is expected that, even before the discharges, flying dust particulates are heated by the weak plasma produced by a tenuous loop voltage induced by the ramp up of the current inside the ohmic transformer [9]. The transformer current ramp starts at −4 s and finishes at −0.8 s before the discharges. A technical description of IR camera setup in AUG can be found in Ref. [16].

Finally, during the AUG summer 2022 shutdown, *dust collection* was carried out by means of a filtered vacuuming technique (Sigma-Aldrich Durapore PVDF® 0.1 μm pore size) in different vessel locations, namely in the mid plane of sectors 3, 10, 16 and below the roof baffle of section 9 (at the inner and outer position). A magnetic dust batch was separated from the collected dust by a permanent magnet. Its morphology and structure was subsequently analyzed. A comparison was carried out with magnetic dust collected from other tokamaks [6,7].

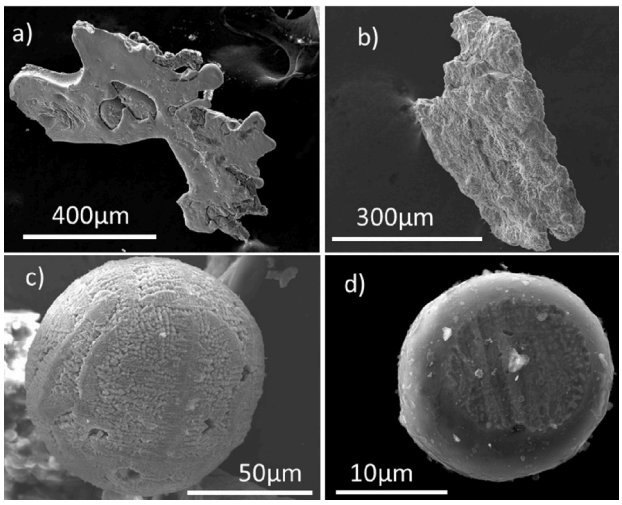

Fig. 2. SEM images of magnetic dust collected from AUG. (a) Ni-based splash (back view), (b) flake (steel), (c) near-spherical dust (steel) with dendrite textured surface, (d) near-spherical dust (steel) without dendrite texture.

Table 1
Chemical composition of the magnetic particulates depicted in Fig. 2, obtained by EDX analysis. Percentage expressed in wt%.

Dust	C	O	Cr	Mn	Fe	Ni	Other
(a)	4.69	4.07	15.4	0.73	8.19	63.5	3.42
(b)	17.7	12.5	–	–	68.1	–	6.87
(c)	2.26	21.9	15.5	–	48.0	7.47	4.87
(d)	2.65	0.93	16.2	–	68.6	9.78	1.84

3. Results

On-line investigation. The analysis of data acquired over ~1300 discharges by the dust optical diagnostic did not reveal clear evidence in favor of the presence of fly-by dust before discharges. Note that the diagnostic was also active during plasma discharges terminating at disruptions, this confirmed its ability to detect the presence of remobilized dust as shown in Fig. 1. Moreover, the analysis of the 196 IR videos acquired with anticipated trigger also revealed no clear evidence of mobile dust before discharges.

Off-line investigation. Dust collected beneath the roof baffle featured a measurable magnetic component, 2wt%, from the total collected dust quantity of 61 mg. SEM and EDX analysis of the AUG magnetic dust showed that the morphology and chemical composition is similar to magnetic dust collected from other tokamaks [6], *i.e.*, spheroids, flakes and splashes mainly composed of nickel or steel compounds, see Fig. 2 and Table 1. The dimensions of spherical dust span up to ~100 μm, whereas flakes and splashes extended up to 1 mm.

The structural investigation of the magnetic and non-magnetic dust batches, carried out by XRD spectroscopy, clearly confirmed that magnetic dust is based on Ni or steel compounds, see Fig. 3a. In contrast to other tokamaks [7], the steel-based magnetic dust in AUG has a ferritic crystal structure with no detectable austenitic features. This confirms the logical expectation that the steel-based AUG magnetic dust primarily originates from the P92 steel tiles. Meanwhile, the non-magnetic dust spectrum, see Fig. 3b, does not feature any peak due to steel or Ni compounds.

4. Discussion

The off-line investigation unambiguously demonstrated the presence of magnetic dust in AUG, albeit in a tiny amount compared to other devices, see Table 2. On the other hand, the on-line investigation did not provide any evidence in favor of the presence of fly-by dust

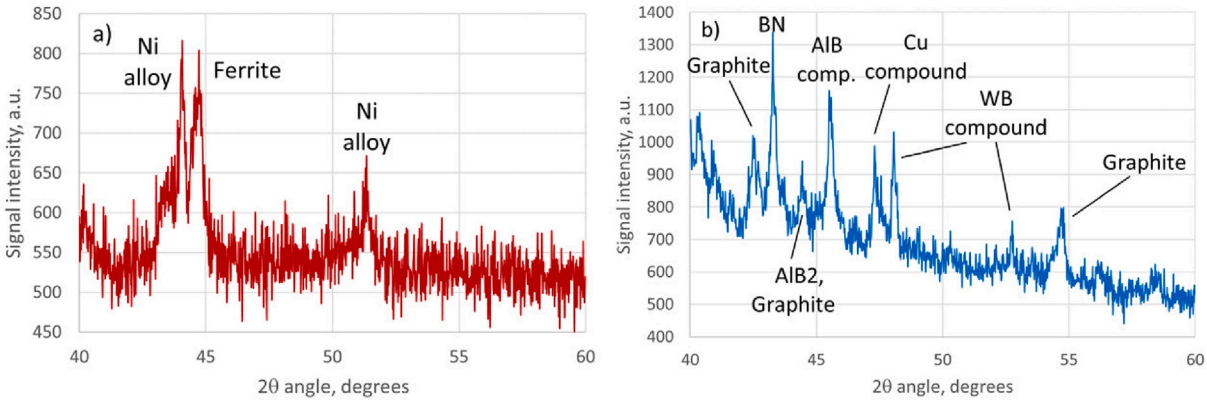

Fig. 3. XRD spectra of the magnetic (a) and non-magnetic (b) dust batches from AUG. It should be noted that the W peaks are located outside the depicted spectral window in order to increase the readability of the most significant spectral range.

before discharges. The possible reasons behind the negative detection of magnetic dust mobilization prior to AUG discharges, could be: (1) a negligible amount of magnetic dust is present in the AUG vessel or most remains entrapped in vessel ravines; (2) the magnetic moment force strength does not suffice to detach adhered magnetic dust, (3) magnetic dust is mobilized well before the plasma discharges and the diagnostic operation windows. Let us discuss each possibility in further detail.

Negligible amount or trapped dust. Systematic dust collection activities have revealed that AUG is characterized by a small dust production rate [17]. In addition, the machine is vacuum cleaned at each shutdown, that is usually planned every year, which includes the removal of the roof baffles. It should also be mentioned that the vessel surface that is covered by P92 steel is 3.46 m^2, to be compared to the entire AUG vessel surface of 32.36 m^2. Finally, magnetic dust was only collected below the divertor (i.e. under the roof baffle), which increases the probability that mobilized magnetic dust would remain trapped locally during the external magnetic field ramp up phase.

Ineffectiveness of magnetic moment force. Pre-plasma magnetic dust detachment is the consequence of the competition between the adhesive force F_{vdW} which is well-described by the van der Waals force [18–20], the magnetic moment force F_{VB} and the gravitational force F_g. These forces are proportional either to the linear dimension (F_{vdW}) or the volume (F_{VB}, F_g) leading to the established conclusion that larger magnetic dust can be easier detached [9]. Neglecting surface roughness and assuming perfectly spherical dust, the normal force balance condition yields a threshold radius above which magnetic dust can be lifted up by the magnetic moment force [9]. In the case of iron grains and at the bottom position ($R = R_0 = 1.56$ m), the threshold radius becomes $\sim 120\,\mu$m for the maximum admissible AUG toroidal field of $B_t = 3$ T. It should be noted that surface roughness would convert this deterministic criterion to a probabilistic criterion allowing the detachment of smaller magnetic dust with a small but finite probability [21,22]. Given the $\sim 50\,\mu$m radius of the largest spherical magnetic dust collected in AUG and considering the fact that AUG was operated below 3 T during the majority of analyzed discharges, it is plausible that the produced magnetic dust is not large enough to be lifted by the external magnetic moment force.

Dust mobilization prior to the diagnostic data acquisition. Fig. 4 features the temporal evolution of the toroidal magnetic field together with the on-line diagnostic acquisition windows in AUG and FTU. It is apparent that AUG acquisition windows cover only the last part of the B_t ramp up phase, while FTU acquisition windows cover a substantially larger portion. This implies that one cannot exclude that magnetic dust mobilization still takes place in AUG, but well before the activation of the relevant diagnostics. In fact, the B_t ramp up phase in AUG is so prolonged that there is ample time for magnetic dust to detach from the low field side, traverse the entire vessel cross-section and re-adhere at the high field side, where the magnetic moment force becomes compressive. In any case, such early instances of pre-plasma dust mobilization would merely constitute a harmless re-distribution of the magnetic dust inventory, since they cannot possibly cause any complications to the plasma start-up.

Table 2
Comparison of the magnetic dust component of AUG with that of other tokamaks [3,6]. Dust amount collected and vessel material composition at the time of collection. See Refs. [3,6] for the dust collection methods and the collection sites.

Tokamak device	Dust collected (gr)	Magnetic dust (wt%)	Wall material	Limiter/ divertor material
FTU	62.85	25.0	SS304 LN	Mo
Alc. C-Mod	0.27	27.4	Mo	Mo
COMPASS	0.238	17.6	Inconel	Graphite
TEXTOR	N/A	15	Graphite	Graphite
AUG	0.06	2	W, P92 steel	W

5. Summary and conclusions

This work presents preliminary results of an experimental study on the realization of magnetic dust mobilization before AUG plasma discharges. The online investigation, based on optical diagnostics and IR camera observations, did not yield any unambiguous detection of such events. On the other hand, the offline investigation, based on the analysis of dust collected after shutdown, proved the presence of magnetic dust. The possible explanations concern the minuscule amount of magnetic dust produced in AUG that could further be efficiently trapped beneath the roof baffle, the ineffectiveness of magnetic moment forces given the produced dust sizes and the operating magnetic fields or the mobilization of magnetic dust well before diagnostic acquisition windows given the prolonged toroidal magnetic field ramp-up phase.

Future AUG investigations should anticipate the trigger of the optical diagnostic −6.5 s before the plasma discharges so that the acquisition window overlaps with the entire temporal evolution of the toroidal magnetic field. In addition, a dust collection activity *during pure magnetic discharges*, *i.e.* with no plasma, at maximum toroidal magnetic field strength should be considered where a dust collector is exposed in the divertor region by means of the X-Point Manipulator insertion system and is later analyzed for the presence of magnetic dust.

Concerning the pre-plasma mobilization of magnetic dust in future fusion reactors, the volumetric magnetic moment force due to the toroidal field should exceed the AUG estimate in compact high field devices such as SPARC [23] but not large size tokamaks such as ITER [24]. Naturally, the mobilizing potential of the magnetic moment force will strongly depend on the magnetic dust sizes that could exceed several hundred microns when generated in the course of melting

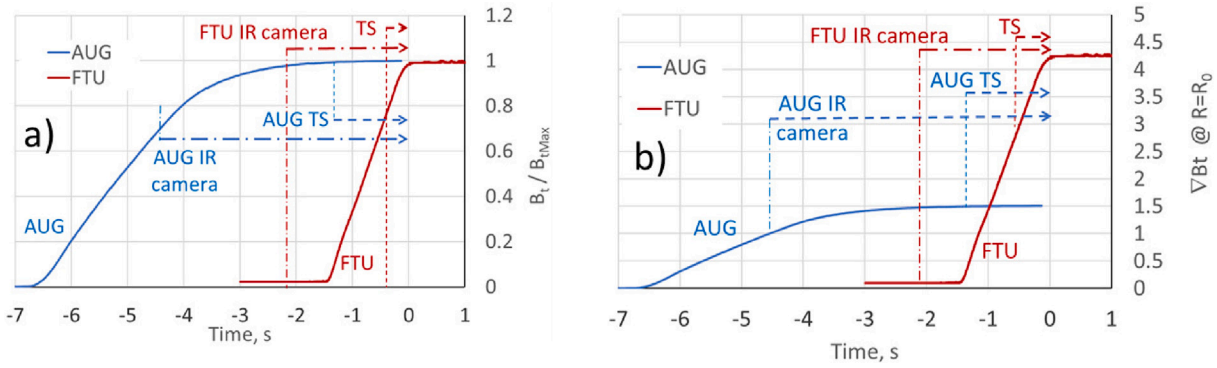

Fig. 4. Temporal evolution of (a) B_t/B_{tMax}, (b) ∇_{B_t} for typical AUG (#40373, blue line) and FTU (#40819, red line) discharges with $B_{tMax}(AUG) = -2.5\,T$ and $B_{tMax}(FTU) = 4\,T$. Note that ∇_{Bt} is evaluated at the low position $R = R_0$ for both devices; $R_0(AUG) = 1.65\,m$ and $R_0(FTU) = 0.935\,m$. (For interpretation of the references to color in this figure legend, the reader is referred to the web version of this article.)

events [2,25]. Finally, it should be noted that, given that new devices work with superconductive magnets that start operating sufficiently well before the plasma discharges, possible issues due to magnetic dust mobilization should not be ascribed to the toroidal field ramp up.

CRediT authorship contribution statement

M. De Angeli: Conceptualization, Methodology, Data analysis, Writing. **V. Rohde:** Validation, Methodology. **P. Tolias:** Conceptualization, Validation, Writing. **S. Ratynskaia:** Conceptualization. **F. Brochard:** Data analysis. **C. Conti:** Resources. **M. Faitsch:** Resources, Investigation. **B. Kurzan:** Resources. **D. Ripamonti:** Resources, Investigation.

Declaration of competing interest

The authors declare the following financial interests/personal relationships which may be considered as potential competing interests: Marco De Angeli reports financial support was provided by European Consortium for the Development of Fusion Energy.

Data availability

The authors do not have permission to share data.

Acknowledgments

This work has been carried out within the framework of the EUROfusion Consortium, funded by the European Union via the Euratom Research and Training Programme (Grant Agreement No 101052200 — EUROfusion). Views and opinions expressed are however those of the authors only and do not necessarily reflect those of the European Union or of the European Commission. Neither the European Union nor the European Commission can be held responsible for them.

References

[1] S. Ratynskaia, et al., Nucl. Mater. Energy 12 (2017) 569.
[2] S. Ratynskaia, et al., Plasma Phys. Control. Fusion 64 (2022) 044004.
[3] J. Winter, Plasma Phys Control. Fusion 40 (1998) 1201.
[4] D. Ivanova, et al., Phys. Scr. T 138 (2009) 014025.
[5] M. De Angeli, et al., Nucl. Fusion 55 (2015) 123005.
[6] M. De Angeli, et al., Fus. Eng. Des. 166 (2021) 112315.
[7] M. De Angeli, et al., Nucl. Mater. Energy 28 (2021) 101045.
[8] H. Pan, et al., Nucl. Mater. Energy 33 (2022) 101251.
[9] M. De Angeli, et al., Nucl. Fusion 59 (2019) 106033.
[10] R.A. Pitts, et al., J. Nucl. Mater. 463 (2015) 748.
[11] K. Sugiyama, et al., Nucl. Mater. Energy 8 (2016) 1.
[12] M. Gorley, et al., Fus. Eng. Des. 170 (2021) 112513.
[13] I. Zammuto, et al., Fus. Eng. Des. 98–99 (2015) 1419.
[14] I. Zammuto, et al., Fus. Eng. Des. 124 (2017) 297.
[15] B. Kurzan, H. Murmann, Rev Sci. Instrum. 82 (2011) 103501.
[16] B. Sieglin, et al., Rev. Sci. Instrum. 86 (2015) 113502.
[17] M. Balden, et al., Nucl. Fusion 54 (2014) 073010.
[18] G. Riva, et al., Nucl. Mater. Energy 12 (2017) 593.
[19] P. Tolias, Fus. Eng. Des. 133 (2018) 110.
[20] P. Tolias, Surf. Sci. 700 (2020) 121652.
[21] P. Tolias, et al., Plasma Phys. Control. Fusion 58 (2016) 025009.
[22] P. Tolias, et al., Nucl. Mater. Energy 15 (55) (2018).
[23] P. Rodriguez-Fernandez, et al., Nucl. Fusion 62 (2022) 042003.
[24] The ITER Organization, ITER research plan within the staged approach, ITER Technical Report ITR-18-003, 2018.
[25] S. Ratynskaia, et al., Rev. Mod. Plasma Phys. 6 (2022) 20.